

NONLINEAR OPTICAL PHENOMENA

PACS numbers: 42.65.Dr; 42.55.Ye; 42.70.Mp
DOI: 10.1070/QE2013v043n07ABEH014996

Four-wave-mixing generation of SRS components in $BaWO_4$ and $SrWO_4$ crystals under picosecond excitation

T.T. Basiev, M.E. Doroshenko, L.I. Ivleva, S.N. Smetanin, M. Jelínek, V. Kubeček, H. Jelínková

Abstract. **Four-wave-mixing stimulated Raman scattering (SRS) generation of Stokes and anti-Stokes components in $BaWO_4$ and $SrWO_4$ crystals excited by a 1064-nm pulsed laser with a pulse duration of 18 ps has been investigated. It is shown that, due to the four-wave mixings of SRS components in short (~1 cm) crystals, the generation thresholds of the second and third Stokes components are much lower than the values determined by the cascade SRS mechanism. If the crystal length is increased by a factor of more than four, the mechanism of multiwave SRS becomes similar to the cascade mechanism (without four-wave mixings). Rotation of $BaWO_4$ crystal makes it possible to control the competition of the processes of four-wave-mixing SRS generation of anti-Stokes and second Stokes components.**

Keywords: *stimulated Raman scattering, four-wave mixing, Stokes and anti-Stokes components.*

1. Introduction

A new wave of interest in solid-state SRS lasers arose in the beginning of the 2000s, when the technology of synthesis and growth of large crystals of barium and strontium tungstates was developed [1–5]. These crystals have high peak and integral SRS amplification cross sections, due to which they can be used to design high-power compact solid-state SRS lasers [6–37]. Cascade generation of high-order SRS components using these crystals (which, in addition, are transparent in a wide wavelength range) may provide further advance into the IR region, up to the transparency edge of active SRS material [23]. However, implementation of cascade generation of higher Stokes components is limited by the decrease in the SRS gain [19] and the radiation resistance threshold of the SRS medium.

One of the ways to implement SRS in the IR spectral region is to narrow the pump pulse width to few picoseconds, due to which the radiation resistance of the SRS medium greatly increases and, therefore, pump intensity can be increased above the threshold at single-pass SRS even for a short piece of medium. In this case, the conditions for four-wave parametric coupling of SRS components can be satisfied and, correspondingly, their generation thresholds can be reduced [38–40]. However, the SRS regime becomes time-dependent, because the pump pulse width is now comparable with the dephasing time of optical phonons; as a result, the SRS generation thresholds increase [16]. These competing processes require detailed analysis in comparative study of multiwave SRS in crystals pumped by picosecond pulses.

In this paper, we report the results of the experimental study of four-wave-mixing SRS generation in barium and strontium tungstate crystals pumped by a 1064-nm picosecond laser.

T.T. Basiev, M.E. Doroshenko, L.I. Ivleva, S.N. Smetanin
A.M. Prokhorov General Physics Institute, Russian Academy of Sciences, ul. Vavilova 38, 119991 Moscow, Russia; e-mail: ssmetanin@bk.ru;
M.Jelínek, V.Kubeček, H.Jelínková Czech Technical University, 11519 Prague, 1, Brehova, 7, Czech Republic

Received 1 August 2012; revision received 4 February 2013
Kvantovaya Elektronika **43** (7) 616–620 (2013)
Translated by Yu.P. Sin'kov

2. Experimental setup

The experimental setup is shown in Fig. 1. $BaWO_4$ and $SrWO_4$ crystals were pumped by a laboratory oscillator–amplifier laser system, emitting at a wavelength λ_L = 1064 nm. A Nd:YAG laser oscillator with quasi-cw diode pumping and passive mode locking by a semiconductor saturable absorber was applied. When using the cavity-dumping technique, the laser oscillator generated single pulses with energy of 20 ± 2 μJ and vertical linear polarisation. The output laser beam had a Gaussian-like profile in both transverse coordinates. The pulse width was measured by a streak camera to be 18 ± 2 ps. A detailed description of the laser system can be found in [41].

A single-pass lamp-pumped Nd:YAG laser amplifier was applied to generate laser pulses of higher energy. The maximum energy of amplified laser pulse at the input of the pumped SRS crystal ($BaWO_4$ or $SrWO_4$) was 2 mJ at a pulse-to-pulse instability of 10%. The laser beam at the amplifier output had a diameter ~1.5 mm, with a quality parameter $M^2 \approx 1.8$. The laser pulse width did not change during amplification. The pulse repetition rate was up to 3 Hz.

To increase the laser intensity, the transverse beam cross section was reduced to 3.1×10^{-3} cm^2 (at the e^{-2} level of maximum intensity) using a telescopic system composed of two collecting lenses: L2 (f = 100 mm) and L3 (f = 50 mm). The SRS radiation spectrum was measured with an Ocean-Optics NIR512 spectrometer (wavelength range 850–1700 nm, resolution 3 nm). The pump laser radiation was transmitted through a silicon wafer filter or a Thorlabs FEL1150 filter. Simultaneously the pump laser pulse energy was precisely measured with a Coherent FieldMax II power and energy meter by deflecting some part of the laser beam using a half-wave plate and polariser mounted at the laser amplifier output.

The $BaWO_4$ and $SrWO_4$ SRS crystals under study were grown at the Scientific Center of Laser Materials and Technologies (Prokhorov General Physics Institute, Russian Academy of Sciences).

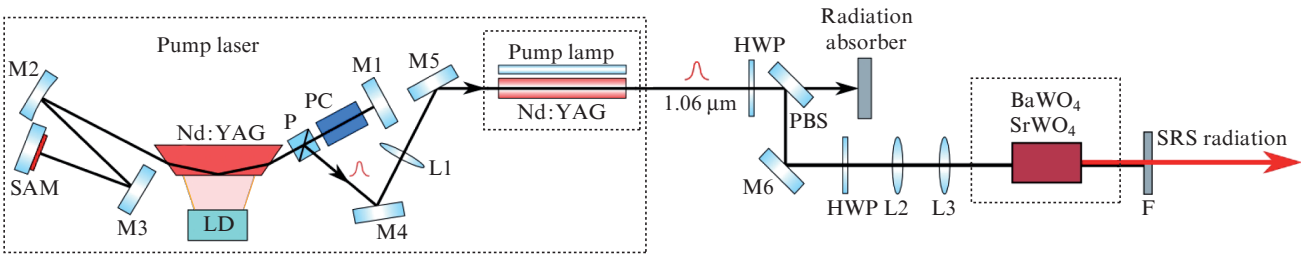

Figure 1. Optical scheme of the experimental setup: (M1–M6) mirrors, (L1–L3) lenses, (SAM) saturable absorber mirror, (PC) Pockels cell, (P) polariser, (HWP) half-wave plate, (PBS) polarisation beam-splitter, (F) filter, and (LD) laser diode.

3. Generation thresholds for the first, second, and third Stokes SRS components in $BaWO_4$ and $SrWO_4$ crystals

$BaWO_4$ and $SrWO_4$ crystals were, respectively, 0.8 and 1.1 cm long in the optical axis direction and had sizes of 1.2 and 4.7 cm in the transverse direction. The crystal end faces were polished to implement pumping in both directions.

In this study we measured the generation thresholds for different SRS components. Note that, although SRS does not have a threshold in the absence of intrinsic loss, in fact, there is an experimental threshold, which is due to the very fast exponential rise in the SRS radiation intensity in the initial stage. For stationary SRS, the increment of this increase is $G_0 = gI_L L$ [11], where g is the SRS gain, I_L is the pump intensity, and L is the interaction length. In the case of time-dependent SRS, the increase in the SRS intensity remains exponential but occurs at a slower rate. For example, in the large-gain limit for a rectangular pump pulse, the exponential increment $G = (4G_0\tau_L/\tau_R)^{1/2}$ [42], where τ_R is the dephasing time of optical phonons and τ_L is the pump pulse width. The experimental SRS threshold is generally determined by the conditions under which pump radiation becomes significantly depleted [3, 11, 43]. It is well known that, for most types of stimulated light scattering (including SRS), the SRS intensity becomes comparable with the pump intensity ($I_S \approx I_L$) at the increment $G \approx 30$, while a decrease in the pump intensity by 20% (with a decrease in G to 24) leads to a decrease in the SRS intensity by a factor of $e^{30}/e^{24} \approx 400$ [43]. The threshold increment G_{th} can be conventionally chosen as 25 [11], a value at which the SRS intensity is lower than the pump intensity by a factor of $e^{30}/e^{25} \approx 100$. Then the experimental SRS threshold can be determined as a value at which the Stokes intensity reaches 1% of the pump intensity. For generality, the SRS generation thresholds for the higher Stokes components can be defined in the same way.

The experimental generation thresholds of SRS components were found by recording the SRS spectrum with simultaneous measurement of the laser pump energy. Increasing the pump energy, we recorded its threshold values W_{th} satisfying the aforementioned criterion. The error in measuring the threshold pump energies for generating SRS components was independent of the pump laser operation instability and was at the level of instrumental error (less than 5%). Note that the error in estimating the intensity threshold (which determines the increment G) depended also on the errors in estimating the transverse beam cross section (~10%) and the pulse width (11%); i.e., the total error in determining the threshold intensity for SRS generation was ~26%.

First we performed pumping along the optical axis c of $BaWO_4$ and $SrWO_4$ crystals ($\boldsymbol{k} \| c$, $\boldsymbol{E} \perp c$). In the $BaWO_4$ crystal the pump threshold energy W_{th1} for generating the first Stokes SRS component with a wavelength $\lambda_1 = 1181$ nm (Raman frequency shift 926 cm^{-1} [4]) was 0.93 ± 0.05 mJ. In the $SrWO_4$ crystal, the generation threshold for the first Stokes component with the wavelength $\lambda_1 = 1178$ nm (Raman frequency shift 921 cm^{-1} [4]) was observed at $W_{th1} = 0.69 \pm 0.04$ mJ.

The pump threshold energy W_{th2} for generating the second Stokes SRS component with the wavelengths $\lambda_2 = 1325$ and 1321 nm was 1.27 ± 0.06 and 0.98 ± 0.05 mJ in the $BaWO_4$ and $SrWO_4$ crystals, respectively. For the third SRS component ($\lambda_3 = 1511$ nm for $BaWO_4$ and 1504 nm for $SrWO_4$), the threshold pump energy $W_{th3} = 1.83 \pm 0.09$ and 1.82 ± 0.09 mJ for the $BaWO_4$ and $SrWO_4$ crystals, respectively.

Then we performed pumping in the direction perpendicular to the optical axis of the $BaWO_4$ (or $SrWO_4$) crystal, with the pump polarised in the direction parallel to the crystal optical axis: $\boldsymbol{k} \perp c$, $\boldsymbol{E} \| c$. In the $BaWO_4$ crystal with a length $L = 1.2$ cm, the threshold pump energies were as follows: $W_{th1} = 0.48 \pm 0.02$ mJ, $W_{th2} = 0.63 \pm 0.03$ major, and $W_{th3} = 1.06 \pm 0.05$ mJ for the SRS generation of the first, second, and third Stokes components, respectively. For the $SrWO_4$ crystal, which was much longer ($L = 4.7$ cm), the threshold pump energies in this pump direction were $W_{th1} = 0.16 \pm 0.01$ mJ, $W_{th2} = 0.36 \pm 0.02$ mJ, and $W_{th3} = 1.44 \pm 0.07$ mJ for the SRS generation of the first, second, and third Stokes components, respectively.

Thus, in the $BaWO_4$ crystal, the sizes of which in both pump directions were close to 1 cm, the threshold pump energies for generating the second Stokes component exceeds that for generating the first Stokes component by less than twice; specifically, by a factor of $W_{th2}/W_{th1} = 1.33–1.36$. For generation of the third Stokes component, the ratio $W_{th3}/W_{th1} = 1.96–2.21$. The ratios of the threshold energies, W_{th2}/W_{th1} and W_{th3}/W_{th1}, turned out to be smaller than those expected from the cascade mechanism of SRS conversion, in which the conditions $W_{th2}/W_{th1} \geqslant 2$ and $W_{th3}/W_{th1} \geqslant 3$ should be satisfied, because generation of the second (third) Stokes component should begin only when the intensity of the first (second) Stokes component reaches the value comparable with the pump intensity (the first Stokes component) [39]. Thus, we can conclude that the effect of four-wave mixings reduces the thresholds for the higher Stokes components in comparison with the values determined by the cascade SRS mechanism.

For the $SrWO_4$ crystal 1.1 cm long, pumped in the direction of its optical axis, the generation thresholds for the second and third Stokes components exceed that for the first Stokes component by factors of 1.4 and 2.6, respectively; i.e., this case is also characterised by the presence of four-wave mixings, which reduce the generation thresholds for higher Stokes SRS components.

4. Analysis of the four-wave-mixing SRS generation of higher Stokes components in $BaWO_4$ and $SrWO_4$ crystals

It was shown in [38, 39] that the decrease in the SRS generation threshold of the second Stokes component can be explained by the presence of partially degenerate four-wave mixing of pump waves, as well as the first and second Stokes components under the conditions of spatially confined phase locking, if $\Delta kL < 300$, where Δk is the wave-vector mismatch for this mixing. The wave mismatch is determined by the expression [39]

$$\Delta k = (n_0 + n_2 - 2n_1)2\pi\lambda_1^{-1} + (n_0 - n_2)2\pi\nu_R, \quad (1)$$

where n_0 is the refractive index of the pump wave; n_1 and n_2 are, respectively, the refractive indices for the first and second Stokes SRS components; and ν_R is the Raman frequency shift. The wave mismatch Δk (1) decreases when the refractive index dispersion decreases and the wavelength λ_1 approaches the zero-dispersion wavelength λ_d. Based on the reference data on the refractive index dispersion for $BaWO_4$ and $SrWO_4$ crystals [9, 20], we obtain $\Delta k \approx 50$ cm^{-1}; then, $\Delta kL \approx 50$ ($L \approx 1$ cm).The analysis performed in [39] showed that at $\Delta kL \approx 50$ the ratios W_{th2}/W_{th1} and W_{th3}/W_{th1} should be ~1.3 and ~2.0, respectively; these values are in good agreement with the experimental results: $W_{th2}/W_{th1} = 1.3-1.4$ and $W_{th3}/W_{th1} = 2.0-2.6$ for $BaWO_4$ and $SrWO_4$ crystals.

When the $SrWO_4$ crystal, 4.7 cm long in the direction perpendicular to its optical axis, is pumped in this direction, the wave mismatch parameter $\Delta kL > 230$; this fact impedes the four-wave coupling of Stokes SRS components [38, 39]. Due to this, only conventional cascade SRS conversion ($W_{th2}/W_{th1} > 2$ and $W_{th3}/W_{th1} > 3$) was experimentally observed.

Figure 2 shows experimental SRS spectra from the $SrWO_4$ crystal 4.7 cm long, $BaWO_4$ crystal 1.2 cm long, and $BaWO_4$ crystal 0.8 cm long, which correspond to generation threshold for the third Stokes SRS component in these crystals.

According to the data in Fig. 2a, in the $SrWO_4$ crystal (which is longer: 4.7 cm), the generation threshold of the third Stokes component is observed when the intensity of the second Stokes component reaches a value comparable with the intensity of the first Stokes component. This is characteristic of the cascade mechanism of SRS conversion without participation of four-wave mixing of SRS components, when each component is generated from the previous SRS component.

It can be seen in Fig. 2b that, when the SRS crystal length is reduced to 1.2 cm, generation of the third Stokes component begins when the intensity of the second Stokes component is still low. This fact confirms the existence of parametric four-wave processes, which reduce the generation thresholds of higher Stokes components [38], at which the frequency conversion into the third Stokes component occurs not only from the second Stokes component (cascade SRS mechanism) but also from the stronger first component (partially degenerate four-wave mixing at SRS) and, possibly, from the pump wave (nondegenerate four-wave mixing at SRS).

Figure 2c demonstrates that in the shortest (0.8 cm) crystal the second and third Stokes components have very similar intensities; i.e., four-wave mixings are so strong in this case that these SRS components are generated jointly from the previous, stronger SRS components (pump and the first Stokes waves).

Note that the generation threshold of the third Stokes component in the short $BaWO_4$ crystal (1.2 cm, Fig. 2b) turned out to be much lower than that in the $SrWO_4$ crystal, which was four times longer (4.7 cm, Fig. 2a): $W_{th3} = 1.06$ mJ against 1.44 mJ. The decrease in the SRS threshold with a decrease in the SRS crystal length demonstrates practical importance of implementing four-wave mixing of SRS components for generating higher Stokes components. In the long $SrWO_4$ crystal the generation threshold of the third Stokes component was found to be anomalously high even for the cascade mechanism of SRS generation: $W_{th3}/W_{th1} = 8.5$ instead of the calculated value of 3.3 at $\Delta kL = 230$ [39]. This fact can be explained as follows: in our experiment the long $SrWO_4$ crystal exhibited, along with the third Stokes component ($\lambda_3 = 1504$ nm), generation of an unknown component at a wavelength of 1673 nm. This component is not the fourth Stokes component with a Raman shift of 921 cm^{-1}, because its wavelength must be larger ($\lambda_4 = 1746$ nm). It can be attributed to the SRS generation of the first Stokes component with an unknown Raman shift of 1594 cm^{-1} (Raman spectra were measured in [4] for shifts less than 1000 cm^{-1}) from the high-intensity component with a wavelength $\lambda_2 = 1321$ nm. Note that with an increase in the pump energy above 1.44 mJ (threshold for the third Stokes component) the intensity of the third Stokes component barely changed and was low even at the maximum pump energy (2 mJ). This is explained by the energy outflow to the simultaneous process of SRS generation at a wavelength of 1673 nm.

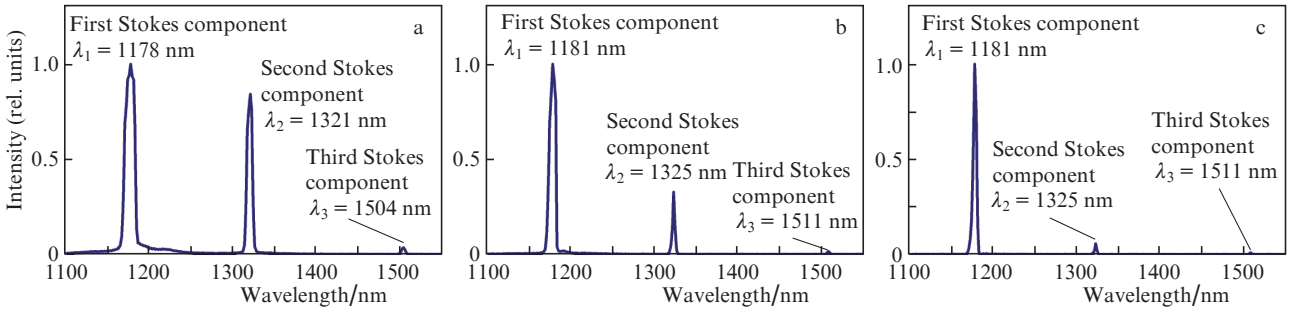

Figure 2. SRS spectra of (a) $SrWO_4$ crystal with $L = 4.7$ cm and $\nu_R = 921$ cm^{-1} and (b, c) $BaWO_4$ crystals with (b) $L = 1.2$ cm and $\nu_R = 926$ cm^{-1} and (c) $L = 0.8$ cm and $\nu_R = 926$ cm^{-1}, corresponding to the generation threshold for the third Stokes SRS component.

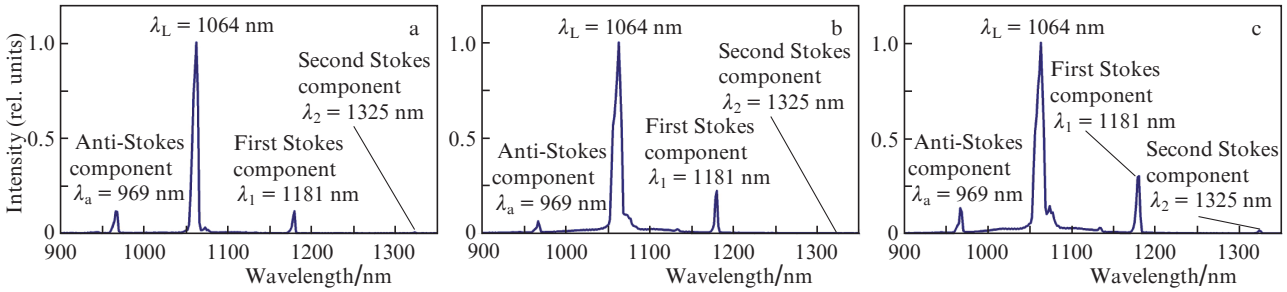

Figure 3. SRS spectra of $BaWO_4$ crystal for pump angles Θ = (a) 0, (b) 20° and (c) 40° at a pump pulse energy of 1.16 mJ.

5. Control of four-wave-mixing SRS generation of the anti-Stokes and second Stokes components during rotation of $BaWO_4$ crystal

Recently we proposed [44] to stimulate four-wave mixings under SRS conditions by orienting a birefringent crystal with respect to the pump direction. In this case, one can reduce and even eliminate the wave phase mismatch Δk of four-wave mixings for the orthogonally polarised SRS components. Here, the four-wave generation of not only higher Stokes but also anti-Stokes components can be optimised.

When using a negative uniaxial $BaWO_4$ crystal, partially degenerate four-wave mixings of ooe type must be optimised [44]; i.e., the wave generated by four-wave mixing (anti-Stokes component or the second Stokes component) must be extraordinary (e), while the other waves involved in this mixing must be ordinary (o).

We performed an experiment on controlling the four-wave-mixing generation of SRS components. To this end, we rotated a crystal with respect to the pump beam direction by an angle Θ. Initially pumping was performed along the optical crystal axis ($\boldsymbol{k} \| c$). The pump radiation was polarised perpendicular to the plane of rotation of crystal; therefore, this radiation was an ordinary wave.

Figure 3 shows the spectra of the SRS components generated in the $BaWO_4$ crystal at different Θ values and pump pulse energy of 1.16 mJ, which is below the generation threshold for the second Stokes component (W_{th2} = 1.27 mJ).

It can be seen in Fig. 3a that at Θ = 0 (i.e., in the case of pumping along the optical crystal axis, efficient four-wave-mixing generation of the anti-Stokes component with a wavelength $\lambda_a = (2\lambda_L^{-1} - \lambda_1^{-1})^{-1}$ = 969 nm and the first Stokes component (λ_1 = 1180 nm) is observed. The anti-Stokes-wave intensity is similar to that for the first Stokes component, and the generation threshold for the second Stokes component was not overcome.

An increase in the angle Θ to 20° (Fig. 3b) leads to a decrease in the anti-Stokes component intensity and an increase in the intensity of the first Stokes component. In addition, the generation threshold of the second Stokes component (λ_2 = 1325 nm) is overcome. A further increase in Θ to 40° (Fig. 3c) results in even more higher intensities of the first and second Stokes components. Unfortunately, an increase in Θ above 40° was limited by the crystal geometry; however, the tendency to increasing the second Stokes component intensity due to energy outflow from the anti-Stokes component is obvious.

Thus, the rotation of $BaWO_4$ crystal made it possible to control the competition of the processes of four-wave-mixing generation of the anti-Stokes component and second Stokes component at SRS. An increase in the angle between the optical crystal axis and pump direction led to a rise in the second Stokes component intensity due to the energy outflow from the anti-Stokes component.

6. Conclusions

We experimentally studied the four-wave-mixing SRS generation of Stokes and anti-Stokes components of radiation in $BaWO_4$ and $SrWO_4$ crystals excited by a 1064-nm pulsed laser with a pulse width of 18 ps. It is shown that, due to the four-wave mixings of SRS components in short (~1 cm) crystals, the generation thresholds of the second and third Stokes components are much smaller than the values determined by the cascade SRS mechanism. When the SRS crystal length increases by a factor of more than four, the mechanism of multiwave SRS becomes similar to the cascade process without four-wave mixings. Rotation of $BaWO_4$ crystal allowed us to control the competition processes of four-wave-mixing SRS generation of the anti-Stokes and second Stokes components.

Acknowledgements. This work was supported in part by the Russian Foundation for Basic Research (Grant No. 13-02-00031) and the Czech Science Foundation (Project No. 102/13/08888S).

References

1. Basiev T.T., Sobol A.A., Zverev P.G., Ivleva L.I., Osiko V.V., Powell R.C. *Opt. Mater*., **11**, 307 (1999).
2. Basiev T.T., Sobol A.A., Zverev P.G., Osiko V.V., Powell R.C. *Appl. Opt*., **38**, 594 (1999).
3. Basiev T.T. *Usp. Fiz. Nauk*, **169**, 1149 (1999).
4. Zverev P.G., Basiev T.T., Sobol' A.A., Skornyakov V.V., Ivleva L.I., Polozkov N.M., Osiko V.V. *Kvantovaya Elektron*., **30**, 55 (2000) [*Quantum Electron*., **30**, 55 (2000)].
5. Basiev T.T., Sobol A.A., Voronko Yu.K., Zverev P.G. *Opt. Mater*., **15**, 205 (2000).
6. Černý P., Zverev P.G., Jelínková H., Basiev T.T. *Opt. Commun*., **177**, 397 (2000).
7. Černý P., Jelínková H. *Opt. Lett*., **27**, 360 (2002).
8. Basiev T.T., Černý P., Jelínková H., Zverev P.G. *IEEE J. Quantum Electron*., **38**, 1471 (2002).
9. Voronina I.S., Ivleva L.I., Basiev T.T., Zverev P.G., Polozkov N.M. *J. Optoelectron. Adv. Mater*., **5**, 887 (2003).
10. Ivleva L.I., Basiev T.T., Voronina I.S., Zverev P.G., Osiko V.V., Polozkov N.M. *Opt. Mater*., **23**, 439 (2003).
11. Ivleva L.I., Basiev T.T., Voronina I.S., Zverev P.G., Osiko V.V., Polozkov N.M. *Opt. Mater*., **23**, 439 (2003).
12. Basiev T.T., Osiko V.V., Prokhorov A.M., Dianov E.M. *Top. Appl. Phys*., **89**, 351 (2003).
13. Černý P., Jelínková H., Zverev P.G., Basiev T.T. *Prog. Quantum Electron*., **28**, 113 (2004).

14. Graham K., Fedorov V.V., Mirov S.B., Doroshenko M.E., Basiev T.T., Orlovskii Yu.V., Osiko V.V., Badikov V.V., Panyutin V.L. *Kvantovaya Elektron*., **34**, 8 (2004) [*Quantum Electron*., **34**, 8 (2004)].
15. Basiev T.T., Gavrilov A.V., Osiko V.V., Smetanin S.N., Fedin A.V. *Kvantovaya Elektron*., **34**, 649 (2004) [*Quantum Electron*., **34**, 649 (2004)].
16. Basiev T.T., Danileiko Yu.K., Doroshenko M.E., Fedin A.V., Gavrilov A.V., Osiko V.V., Smetanin S.N. *Laser Phys*., **14**, 917 (2004).
17. Basiev T.T., Zverev P.G., Karasik A.Ya., Osiko V.V., Sobol' A.A., Chunaev D.S. *Zh. Eksp. Teor. Fiz*., **126**, 1073 (2004).
18. Basiev T.T. *Fiz. Tverd. Tela*, **47**, 1354 (2005).
19. Lisinetskii V.A., Rozhok S.V., Bus'ko D.N., Chulkov R.V., Grabtchikov A.S., Orlovich V.A., Basiev T.T., Zverev P.G. *Laser Phys. Lett*., **2**, 396 (2005).
20. Ge W., Zhang H., Wang J., Liu J., Li H., Cheng X., Xu H., Hu X., Jiang M. *J. Cryst. Growth*, **276**, 208 (2005).
21. Chen Y.F., Su K.W., Zhang H.J., Wang J.Y., Jiang M.H. *Opt. Lett*., **30**, 3335 (2005).
22. Jia G., Tu C., Brenier A., You Z., Li J., Zhu Z., Wang Y., Wu B. *Appl. Phys. B*, **81**, 627 (2005).
23. Basiev T.T., Basieva M.N., Doroshenko M.E., Fedorov V.V., Osiko V.V., Mirov S.B. *Laser Phys. Lett*., **3**, 17 (2006).
24. Ling Z.C., Xia H.R., Ran D.G., Liu F.Q., Sun S.Q., Fan J.D., Zhang H.J., Wang J.Y., Yu L.L. *Chem. Phys. Lett*., **426**, 85 (2006).
25. Basiev T.T., Doroshenko M.E., Ivleva L.I., Osiko V.V., Kosmyna M.B., Komar V.K., Šulc J., Jelínková H. *Kvantovaya Elektron*., **36**, 720 (2006) [*Quantum Electron*., **36**, 720 (2006)].
26. Basiev T.T., Osiko V.V. *Usp. Khim*., **75**, 939 (2006).
27. Basiev T.T., Vodchits A.I., Orlovich V.A. *Opt. Mater*., **29**, 1616 (2007).
28. Doroshenko M.E., Basiev T.T., Vassiliev S.V., Ivleva L.I., Komar V.K., Kosmyna M.B., Jelínková H., Šulc J. *Opt. Mater*., **30**, 54 (2007).
29. Šulc J., Jelínková H., Basiev T.T., Doroshenko M.E., Ivleva L.I., Osiko V.V., Zverev P.G. *Opt. Mater*., **30**, 195 (2007).
30. Piper J.A., Pask H.M. *IEEE J. Sel. Top. Quantum. Electron*., **13**, 692 (2007).
31. Li S., Zhang X., Wang Q., Zhang X., Cong Z., Zhang H., Wang J. *Opt. Lett*., **32**, 2951 (2007).
32. Jia G., Wang H., Lu X., You Z., Li J., Zhu Z., Tu C. *Appl. Phys. B*, **90**, 497 (2008).
33. Fan Y.X., Liu Y., Duan Y.H., Wang Q., Fan L., Wang H.T., Jia G.H., Tu C.Y. *Appl. Phys. B*, **93**, 327 (2008).
34. Fan L., Fan Y.X., Duan Y.H., Wang Q., Wang H.T., Jia G.H., Tu C.Y. *Appl. Phys. B*, **94**, 553 (2009).
35. Basiev T.T., Basieva M.N., Gavrilov A.V., Ershkov M.N., Ivleva L.I., Osiko V.V., Smetanin S.N., Fedin A.V. *Kvantovaya Elektron*., **40**, 710 (2010) [*Quantum Electron*., **40**, 710 (2010)].
36. Lee A.J., Pask H.M., Piper J.A., Zhang H., Wang J. *Opt. Express*, **18**, 5984 (2010).
37. Xu H., Zhang X., Wang Q., Wang C., Wang W., Li L., Liu Z., Chong Z., Chen X., Fan S., Zhang H., Tao X. *Appl. Phys. B*, **107**, 343 (2012).
38. Basiev T.T., Smetanin S.N., Fedin A.V., Shurygin A.S. *Opt. Spektrosk*., **107**, 377 (2009).
39. Basiev T.T., Smetanin S.N., Shurygin A.S., Fedin A.V. *Usp. Fiz. Nauk*, **180**, 639 (2010).
40. Shen Y.R. *The Principles of Nonlinear Optics* (New York: Wiley, 1984; Moscow: Nauka, 1989).
41. Jelínek M., Kubeček V. *Laser Phys. Lett*., **8**, 657 (2011).
42. Carman R.L., Shimizu F., Wang C.S., Bloembergen N. *Phys. Rev. A*, **2**, 60 (1970).
43. Zel'dovich B.Ya., Pilipetskii N.F., Shkunov V.V. *Principles of Wave Conjugation* (Berlin: Springer-Verlag, 1985; Moscow: Nauka, 1985).
44. Smetanin S.N., Basiev T.T. *Kvantovaya Elektron*., **42**, 224 (2012) [*Quantum Electron*., **42**, 224 (2012)].